Characteristics of a series of high speed hard chine planing hulls – Part 1: Performance in calm water.

D.J. Taunton, Fluid-Structure Interaction Research Group, School of Engineering Sciences, University of Southampton
D.A. Hudson, Fluid-Structure Interaction Research Group, School of Engineering Sciences, University of Southampton
R.A. Shenoi, Fluid-Structure Interaction Research Group, School of Engineering Sciences, University of Southampton

SUMMARY

A new series of high speed hard chine planing hulls was designed to study their performance in both calm water and waves. This study was undertaken to determine the influence of hull design parameters such as length-displacement ratio, static trim angle and radius of gyration on the performance of the people on board these craft when travelling at high speed in waves. The series designed extends the speed range for which data are available for planing hulls.

This study summarises the calm water performance of the vessels. Resistance, dynamic trim angle and dynamic sinkage are measured for the series and presented together with an uncertainty analysis of the experimental data. The dynamic wetted surface area of each hull was determined and is included in the data presented. An example of the standard ITTC scaling procedure for high speed marine vehicles is given with a discussion of the impact of including spray resistance using Savitsky's whisker spray drag formulation.

NOMENCLATURE

β	Deadrise [^{o}]
Δ	Displaced weight [N]
θ_V	Dynamic trim angle [degrees]
∇	Displaced volume [m^3]
λ	Ship scale factor
B	Beam [m]
C_Δ	Load Coefficient = $\Delta/(g\ \rho\ B^3)$
Cv	Speed coefficient =$V/(gB)^{0.5}$
Fr_L	Length Froude Number = $V/(g\ L)^{0.5}$
Fr_∇	Volumetric Froude number = $V/(g\ \nabla^{1/3})^{0.5}$
G	Acceleration due to gravity 9.80665m/s^2
L	Length over all [m]
L_C	Wetted chine length from transom [m]
L_K	Wetted keel length from transom [m]
L_M	Mean wetted length [m]
LCG	Longitudinal centre of gravity [%L] from transom
R_*	Resistance component [N]
Re	Reynolds' Number
S_V	Dynamic Wetted surface area [m^2]
T	Draught [m]
V	Speed [m/s]
Z_v	Dynamic sinkage at LCG [m]

1 INTRODUCTION

In recent years the operation of high speed planing craft for military, commercial and leisure use has increased. With the development of light weight engines and propulsion systems typical operating speeds are now higher. Research into materials and structures has led to the development of stronger hulls, often making the limiting factor for operation the people onboard these craft. Surveys of the operators of high speed craft, including the one carried out by the US Navy into their special forces has shown a high probability of serious injury [1].

The current study forms part of a wider investigation into the influence of typical hull design parameters on the resistance, seakeeping and performance of the people on board these craft in waves. Such design parameters include the slenderness ratio ($L/\nabla^{1/3}$), longitudinal centre of gravity, load coefficient and radius of gyration, together with design features such as transverse steps. As such the data acquisition and signal processing requirements are scaled from full scale requirements for human factors measurements, such as those described in BS ISO 18431 [2], British Standard 6841 [3] and ISO Standard 2631 [4]. These are consistent with a recent summary document produced specifically for small, high speed craft [5].

This paper presents the calm water performance data for a new series of high speed hard chine planing hulls. The design of the hulls is described, together with the experimental investigation undertaken. Data for resistance, dynamic sinkage, dynamic trim angle and dynamic wetted surface area are presented in a format suitable for use by designers of such vessels. A full uncertainty analysis of the experimental data is included. Components of resistance are illustrated for one of the models in the series, in order to aid scaling of these data. A worked example is also included, scaling the model data obtained from these experiments to full scale and highlighting the influence of considering the whisker spray drag for planing craft.

2 DESCRIPTION OF MODELS

Experimental data for the calm water performance of systematic series of high speed planing craft are limited and include Series 62 [6], Series 65 [7] and more recently a series based on the US Coast Guard 47ft Motor Lifeboat (MLB) [8]. The availability of seakeeping data for systematic series of high speed planing craft is even more limited. The most significant series is the prismatic hull series tested by Fridsma

[9, 10] and extended by Zarnick [11]. Other tests of high speed planing craft in waves include those carried out by Rosen and Garme [12-14]. The models tested in these calm water resistance and seakeeping tests are either prismatic forms, or are not representative of modern high speed hull forms. In light of this a new series of hull forms was designed specifically for this investigation.

In order that this series be representative of modern design practice, a survey of built high speed military and para-military interceptor craft and Union Internationale Motonautique (U.I.M) Powerboat P1 boats was undertaken. This survey, summarised in table 1, shows that typical L/B values range from 3.7 to 5.8. These parameters were borne in mind when designing the series described here.

Vessel	LOA [m]	B [m]	T [m]	L/B
Chaudron 33	10.1	2.2	-	4.6
CMN Interceptor DV15	15.5	3.0	0.8	5.2
Damen Interceptor 1202	11.6	2.5	1.7	4.7
Damen Interceptor 1503	15.0	2.7	1.7	5.6
Damen Interceptor 2004	20.0	4.5	2.5	4.4
Damen Interceptor 2604	26.1	6.0	3.1	4.4
Donzi 38 ZR Comp	11.6	2.8	0.7	4.1
Dragon 39	11.9	2.6	0.9	4.6
FB 42' poker run	12.9	2.6	-	5.0
FB 48 STAB	12.8	3.1	-	4.2
FB Design FB38	11.9	2.3	-	5.1
FB Design FB42	13.0	2.6	1.0	4.9
FB Design FB55	16.6	2.9	1.2	5.8
FB Design FB80	24.0	6.0	-	4.0
Formula 382 FASTECH	11.6	2.5	0.8	4.6
Fountain Lightning 42	12.8	2.6	1.0	4.9
Hustler 388 Slingshot	11.8	2.6	-	4.5
Metamarine TNT 46 Corsa	14.6	2.8	0.6	5.2
Rodriguez V6000	16.5	2.8	-	5.8
Storebro 90E	10.8	2.9	0.7	3.7
Sunseeker XS Sport	11.9	2.3	0.8	5.1
VT Enforcer 33	10.1	2.6	0.7	3.9
VT Enforcer 40	12.2	2.7	0.8	4.4
VT Enforcer 46	13.9	2.8	0.9	5.0

Table 1: Survey of Interceptor and P1 boat dimensions.

Details of the model series designed for this study are shown in table 22. The body plan and profile of the models in the series are shown in figure 1 and 2, respectively. Variants of model C having one and two transverse steps are designated as models C1 and C2, respectively. These steps are perpendicular to the centreline of the models, as shown in figure 2.

All of the models were constructed from foam and painted with primer before being sanded with 800g/m^2 wet and dry paper. A maximum model weight of 50 percent of the displacement was specified in order to ballast the models to achieve the required pitch radius of gyration for subsequent testing in head waves.

The parent hull, designated model C, is typical of high speed interceptor craft and race boats. The model has a L/B ratio of 4.3 and a transom deadrise angle of 22.5^o. The hullform was modified to remove the two transverse steps and the two spray rails often seen on such craft.

The variation in L/B ratio and speeds tested for the developed model series are compared to previous experimental investigations of planing craft performance in table 3. It may be seen that the experiments conducted extend the speed range for which data are available.

Model	A	B	C	D
L[m]	2.0	2.0	2.0	2.0
B[m]	0.32	0.39	0.46	0.53
T[m]	0.06	0.08	0.09	0.11
Δ[N]	119.25	175.83	243.40	321.95
$L/\nabla^{1/3}$	8.70	7.64	6.86	6.25
L/B	6.25	5.13	4.35	3.77
$\beta[^O]$	22.5	22.5	22.5	22.5
LCG [%L]	0.33	0.33	0.33	0.33

Table 2: model details.

The models were towed by a single free-to-heave post, with yaw restraint, attached at the longitudinal centre of gravity by a free-to-pitch fitting. All models were towed from a height of 1.1 times the draught above the keel (i.e. 1.1T). As the models are not representative of a particular vessel, the propulsor was not known. It was therefore assumed that the thrust line passed through the centre of gravity and that the thrust acts horizontally. No correction moment was therefore applied to correct for the thrust lever. The models were tested at a number of static trim angles.

Similarly, without a full-scale design length or speed, it was not possible to apply a correction moment for the skin friction resistance (δR_F).

3 FACILITIES AND TESTS

3.1 FACILITIES

All of the experiments were conducted in the GKN Westland Aerospace No.3 Test Tank, at their test facilities in Cowes on the Isle of Wight. The tank has the following principal dimensions:

Length: 198m

Breadth: 4.57m

Depth: 1.68m

Maximum Carriage Speed: 15m/s

The tank has a manned carriage on which is installed a dynamometer for measuring model total resistance together with various computer and instrumentation facilities for automated data acquisition.

3.2 INSTRUMENTATION AND MEASUREMENTS

The resistance of the model was measured with a force block dynamometer mounted between the fitting in the model and the tow post. Dynamic sinkage at the centre of gravity was measured with a rotary potentiometer attached by a gear to a track on the free to heave tow post. The tow post was mounted at the longitudinal centre of gravity of the model. The trim angle was measured with a rotary potentiometer in the tow fitting. The longitudinal acceleration of the towing carriage was measured using a piezoresistive accelerometer [CFX USCA-TX, Range 10g] mounted on the carriage. This enabled the constant speed run section to be detected during the analysis in order to maximise the run length, as illustrated in figure 3.

All data signals were acquired using a high speed data logger [IOTECH DaqLab 2001] at a sample rate of 5000Hz and stored on a laptop PC. Four pole Butterworth anti-aliasing filters with a cut off frequency of 2000Hz for the accelerations and 200Hz for all other signals were employed. The sample rate and anti-aliasing filter frequencies were selected for the subsequent seakeeping experiments, based on nominal full scale requirements [15]. The time base was scaled from full scale to model scale for a nominal scale factor of λ=5.435, with the resulting factor being rounded to two for convenience.

3.3 TEST PROCEDURES

The models were tested in calm water at speeds from 4 to 12m/s. Measurements of model dynamic sinkage, trim angle and resistance were made. In addition photographs and video of the run were used to identify the dynamic wetted surface area. In accordance with ITTC Recommended Procedures on boundary layer turbulence stimulation [16], no stimulation was applied to the model as all but the lowest speed tested (4 m/s) resulted in a Reynolds' number higher than the critical Reynolds' number of $5x10^6$.

Each run commenced with the recording of zero levels for every transducer. The carriage was then accelerated down the tank to the required speed. The carriage speed was determined from the time taken to pass through a 15.24m (50ft) section of the tank with automatic timing triggers at the beginning and end. At the end of the run beaches at the side of the tank were automatically lowered to calm the tank. Adequate time for the waves in the tank to settle was left between runs. This averaged out at a time of 12 minutes between runs.

4 RESULTS

Calm water resistance is presented graphically (figures 5 to 10) in the non-dimensional form of resistance divided by displacement weight in Newtons (R_T/Δ). The dynamic sinkage is non-dimensionalised by the cube root of displacement volume ($Z_V/\nabla^{1/3}$) and presented in figures 11 to 16. Dynamic trim angle is presented (figures 17 to 22) in degrees and the dynamic wetted surface area is non-dimensionalised by displacement volume to the power of two thirds ($S_V/\nabla^{1/3}$) and shown in figures 23 to 28. All values are plotted against volumetric Froude number. In order to present these data in a format useful for designers and to retain maximum accuracy, tables 4 to 10 present all of the dimensional experimental data for models A,B,C,D,C1 and C2, respectively.

An uncertainty analysis has been conducted using the method described in [17] and using a 95% confidence limit. The results are presented as percentage uncertainty in tables 4 to 10. Some of the data in these tables are presented without uncertainty due to loss of the data files, which prevented an analysis, but it is expected that the uncertainty would be similar to the other conditions since the setup was identical.

Recommended ITTC resistance coefficients are determined in order to illustrate a scaling procedure implementing Savitsky's formulation for whisker drag [18].

4.1 RESISTANCE

The calm water resistance of models A,B,C,D,C1 and C2 is presented in figures 5 to 10, respectively. These illustrate that the R_T/Δ is approximately the same for models A to D. This is reinforced in figure 29 which shows the influence of $L/\nabla^{1/3}$ on resistance, although in general resistance is decreased with decreasing $L/\nabla^{1/3}$. The total resistance of models C1 and C2 is reduced as a result of the reduced wetted surface area caused by the transverse steps.

This influence of the transverse steps on resistance compared with the parent hull is shown in Figure 33. This shows a significant reduction in resistance as speed increases for the stepped hull models. Interestingly, there is no significant difference between the single step and double step. It is worth noting that model C1 was the only model to show signs of porpoising (at a speed of 10m/s). The reason for this is unclear, since the run condition lies outside the expected porpoising limits as depicted in Savitsky [19].

The influence of increasing the load coefficient can be seen in figure 37. Model C has a load coefficient of 0.25 and model C+ represents an increased displacement, with a load coefficient of 0.30. This indicates that there is an inverse relationship between load coefficient and R_T/Δ.

4.2 DYNAMIC SINKAGE

The dynamic sinkage of models A, C, D, C1 and C2 is presented in figures 11 to 16, respectively. The influence of $L/\nabla^{1/3}$ on dynamic sinkage is shown in Figure 30 and illustrates that the non-dimensional sinkage increases with

$L/\nabla^{1/3}$. Results for model B are omitted since valid data were not recorded due to a faulty sensor.

Figure 34 shows that there is no significant influence of transverse steps on the dynamic sinkage. Figure 38 indicates that as load coefficient increases the non-dimensional sinkage ($Z_V/\nabla^{1/3}$) increases by a small amount.

4.3 DYNAMIC TRIM

The dynamic trim of models A,B,C,D,C1 and C2 is presented in figures 17 to 22, respectively. The influence of model, or $L/\nabla^{1/3}$, on dynamic trim is shown in Figure 31. This shows that the dynamic trim angle increases with reducing $L/\nabla^{1/3}$. This is to be expected given the smaller wetted surface area as $L/\nabla^{1/3}$ reduces.

The influence of transverse steps and load coefficient on dynamic trim are shown in figures 35 and 39, respectively. These figures indicate that there is little influence of transverse steps on the dynamic trim angle and that a higher load coefficient increases the dynamic trim angle in a speed range approximately $3.5< Fr_\nabla <5.5$.

4.4 WETTED SURFACE AREA AND SCALING

One of the most difficult parameters to determine experimentally for planing craft is the dynamic wetted surface area. There is no universal, or recommended, method that may be applied [16], yet its determination is critical if scaling from model to full scale is to be achieved and power predicted accurately. Methods to determine dynamic wetted surface area vary from visual observations of the points where the flow separates from the hull (transom immersion, spray root line crossing chine edge and keel) to underwater video use.

The dynamic wetted surface area (aft of the spray root line) was determined from photographs of the model taken during each run. Wetted surface areas for models A,B,C,D,C1 and C2 are presented in figures 23 to 28, respectively. Figure 32 shows that non-dimensional wetted surface area reduces with reducing $L/\nabla^{1/3}$.

Scaling of resistance data from model to full scale may also be undertaken by different methods and again there is no universal or recommended procedure [16]. These methods, although all based on Froude scaling, differ in the manner in which they include whisker spray in the dynamic wetted surface area and the flow direction – hence shear stress on the hull – in the different regions of the wetted surface area. The behaviour of spray is also affected by the surface tension of the water, which leads to different behaviour of spray at model and full scale. In general the spray at model scale forms a more continuous body of water, whereas at full scale it tends to break into smaller droplets of water. As described, in this investigation the dynamic wetted surface area was determined from photographs of the model taken during each run. The wetted surface area was divided into a 'whisker spray region' and a 'pressure wetted area' in the manner of Savitsky [18]. However, whereas Savitsky defines the front of the whisker spray region relative to the spray root line, in the present work it is determined directly from the photographs. A representative pair of photographs is shown in figure 4. The image on the left is used to identify the locations where the spray root line and the whisker spray cross the chine edge. The image on the right is used to identify the location where the water contacts the keel. Similar images were used for all runs. The onset flow is assumed to be reflected about the spray root line, to give the flow direction in the whisker spray region. Determination of the spray drag according to [18] allows a spray drag coefficient to be calculated.

ITTC resistance coefficients for model C are presented in figure 41. Individual resistance components are determined using the method of Savitsky [18]. The frictional resistance coefficient is obtained from the ITTC 1957 skin friction line, using the Reynolds' number based on the mean dynamic wetted length.

In line with recommended ITTC procedures [16] the air resistance of the model is calculated. The air resistance is calculated assuming a drag coefficient of 0.7 and the model frontal area, as suggested in [18]. C_D is the horizontal component of the lift vector calculated using Savitsky's method [18]. Figure 41 illustrates that spray drag becomes significant above a speed of $Fr_\nabla=5.0$. Explicit inclusion of the spray drag term improves agreement between a summation of resistance components and the measured total resistance, although a discrepancy still remains.

5 SCALING EXAMPLES

An example of how to scale the data presented in this paper to full scale is included below. This example uses a geometrically similar full-scale vessel of model C2 with a scale factor $\lambda=7.5$ and hence a length of 15m. The vessel design speed is 64 knots.

5.1 CONVENTIONAL FROUDE SCALING WITH AIR RESISTANCE

In scaling model data for planing craft, the 'residuary' resistance may be determined through subtraction of the frictional and air resistance components from the total resistance of the model. A form factor is not generally applied, nor recommended, due to the difficulties in determining a suitable value with separated flow regimes [16].

a) Total resistance of model C2 from table 9:

   $R_{TM}=83.55$ N

b) Determine the total resistance coefficient for the model:

   $C_{TM}= 0.0032$

c) Determine the frictional resistance coefficient for the model using the ITTC 1957 formula and the mean wetted length, Lm, from table 9:

C_{FM}=0.0030

d) Determine the air resistance coefficient for the model:

R_{AAM}=5.14 N

C_{AAM}=0.0001967

e) Determine the residuary resistance for the ship:

C_R= 7.15 x 10^{-6}

f) Determine the frictional resistance coefficient for the ship using the ITTC 1957 formula:

C_{FS}=0.0019

g) Determine the air resistance coefficient for the ship (assuming same drag coefficient and non-dimensional frontal area at full scale as model. If actual frontal area and drag coefficient are known they should be used here):

R_{AAS}=2169 N

C_{AAS}=0.000192

h) Determine the total resistance coefficient for the ship:

C_{TS}=0.0021

i) Determine the total resistance for the ship:

R_{TS}=23761 N

The example has been included to illustrate the difficulties associated with implementing the standard ITTC high speed marine vehicles scaling procedure. This procedure results in a residuary resistance coefficient C_R that is very small. The whisker spray resistance calculated using Savitsky's method [18] gives a values C_{SM}=0.00033. If this is included in the calculation, the resulting value of C_R is negative. Since this is unrealistic, one of the resistance components may be too large. That is, either the frictional or air resistance coefficient may be too large. The former depends on the calculation of Reynolds' number using the mean wetted length and is relatively insensitive to small changes in this length. The suitability of the ITTC 1957 skin friction correlation line may be questioned for such high speed vessels, given its derivation for conventional merchant ship scaling (although it is recommended in [16] for high speed craft). Using the Schoenherr method to determine skin friction resistance does reduce the skin friction coefficient but only by a very small amount.

The air resistance coefficient is based on an assumed air drag coefficient of 0.7 (as suggested in [16]). This could be a source of error, but it is again unlikely to make sufficient difference to the results given the size of the air resistance component.

Alternatively, the total resistance coefficient as calculated from the measured total resistance may be too small. This depends on the dynamic wetted surface area – which is the measured quantity with the greatest uncertainty (tables 4 to 10). However, if the maximum calculated uncertainty is applied to the wetted surface area in this example (~10%), the change in total resistance coefficient, together with the attendant changes in air and spray drag coefficients, does not result in a significantly greater residuary resistance coefficient. The explicit inclusion of spray drag still results in a negative value of this coefficient. Further study of the components of resistance of planing craft at both model and full scale is thus required.

It should also be noted that the principal particulars of this standard series, including the highest test speeds, lie outside the range of parameters used by Savitsky in deriving the whisker spray drag formulation [18]. It is unclear what effects this may have had on the calculation of spray drag coefficient for this series – although as observed in section 4.4 the inclusion of spray drag appears to improve the calculation of total resistance from its constituent components.

6 CONCLUSIONS

A new series of hard chine planing hulls has been developed to investigate the performance of modern high speed vessels in calm water and waves. The influence of length-displacement ratio on the resistance, sinkage, trim angle and wetted surface area are investigated for a wider range of speeds than previous studies. Furthermore, the influence of altering static trim and load coefficient are included for some models in the series. The influence of transverse steps on the performance characteristics of the parent model is presented and shown to result in a significant reduction in resistance, for either a single or double step. An uncertainty analysis is included with the data.

Dynamic wetted surface areas determined by visual observation are presented for all conditions and shown to decrease with speed for all length-displacement ratios and to decrease with length-displacement ratio.

The inclusion of a whisker spray drag term, as initially presented by Savitsky [18], is shown in an investigation of the components of resistance for the parent hull. This spray drag term is significant at speeds higher than Fr_∇=5.0. Summation of individual components of resistance compared to total resistance is greatly improved through inclusion of the spray drag term, although there is still a discrepancy.

In order to demonstrate the application of the data presented, examples are given for scaling from model to a nominal full scale vessel both with and without the explicit inclusion of a

spray drag term. Difficullties remain with including spray drag in the analysis using the method of Savitsky [18].

The data presented provide a foundation for studying the performance of modern, high speed planing hulls in calm water and waves as well as providing valuable design data absent in the literature.

7 ACKNOWLEDGEMENTS

The work presented herein was funded through the Engineering and Physical Sciences Research Council (EPSRC) under grant no. EP/C525728/1: 'Design of High Performance Craft from a Human Factors Perspective'. The authors would also like to thank Mr. Rasmus Isaksen for his assistance with the tank testing and data analysis.

8 REFERENCES

[1] W. ENSIGN, J. A. HODGDON, W. K. PRUSACZYK, D. SHAPIRO, and M. LIPTON, 'A Survey of Self-Reported injuries Among Special Boat Operators', Naval Health Research Center, Report No. 00-48, 2000.

[2] BRITISH STANDARDS INSTITUTION, 'Mechanical Vibration and Shock - Signal Processing - Part 1: General introduction.', BS ISO 18431-1:2005.

[3] BRITISH STANDARDS INSTITUTION, 'Measurement and evaluation of human exposure to whole-body mechanical vibration and repeated shock.', BS 6841:1987.

[4] INTERNATIONAL ORGANISATION FOR STANDARDISATION, 'Mechanical vibration and shock - Evaluation of human exposure to whole-body vibration -Part 1: General requirements.', ISO 2631-1:1997(E).

[5] T. GUNSTON, 'Draft measurement methodology for small high speed craft – UK view', in *AABCD High Speed Boat Shock & Vibration Measurement Workshop*, RINA Headquarters, London, 2007.

[6] E. P. CLEMENT and D. L. BLOUNT, 'Resistance tests of a systematic series of planing hull forms', *Transactions of The Society of Naval Architects and Marine Engineers, Volume 71*, 1963.

[7] H. D. HOLLING and E. N. HUBBLE, 'Model resistance data of Series 65 hull forms applicable to hydrofoils and planning craft', Naval Ship Research and Development Center, Bethesda., Report No. DTNSRDC 4141, 1974.

[8] B. J. METCALF, L. FAUL, E. BUMILLER, and J. SLUTSKY, 'Resistance tests of a systemetic series of U.S. Coast Guard planing hulls', Carderock Division, Naval Surface Warefare Center, Report No. NSWCCD-50-TR-2005/063, 2005.

[9] G. FRIDSMA, 'A systematic study of the rough-water performance of planing boats', Stevens Institute of Technology, Report No. 1275, 1969.

[10] G. FRIDSMA, 'A systematic study of the rough-water performance of planing boats (Irregular Waves - Part II)', Stevens Institute of Technology, Report No. 1495, 1971.

[11] E. E. ZARNICK and C. R. TURNER, 'Rough water performance of high length to beam ratio planing boats', David W. Taylor Naval Ship Research and Development Center, Bethesda, Maryland, Report No. DTNSRDC/SPD-0973-01, 1981.

[12] K. GARME and J. HUA, 'A method to analyse seakeeping model measurements in time domain', in *Proceedings of the Ninth International Offshore and Polar Engineering Conference (ISOPE-99)*. J. S. Chung, M. Olagnon, C. H. Kim, and A. Francescutto, Eds., 1999, pp. 629-634.

[13] A. ROSEN, 'Loads and responses for planing craft in waves', in *Division of naval Systems, Aeronautical and Vehicle Engineering*. PhD Stockholm: KTH, 2004.

[14] A. ROSEN and K. GARME, 'Model experiment addressing the impact pressure distribution on planing craft in waves', *Transactions of the Royal Institution of Naval Architects, Volume 146*, 2004.

[15] D. P. ALLEN, D. J. TAUNTON, and R. ALLEN, 'A study of shock impacts and vibration dose values onboard highspeed marine craft', *International Journal of Maritime Engineering, Volume 150, pp. 10*, 2008.

[16] INTERNATIONAL TOWING TANK CONFERENCE, 'Testing and Extrapolation Methods, High Speed Marine Vehicles, Resistance Test', in *ITTC - Recommended Procedures and Guidelines*, 2002, p. 18.

[17] K. M. FORGACH, 'Measurement Uncertainty Analysis of Ship Model Resistance and Self Propulsion Tests', Naval Surface Warfare Center, Report No. NSWCCD-50-TR--20002/064, 2002.

[18] D. SAVITSKY, M. F. DELORME, and R. DATLA, 'Inclusion of whisker spray drag in performance prediction method for high-speed planing hulls', *Marine Technology, Volume 44, pp. 35-56*, 2007.

[19] D. SAVITSKY, 'Hydrodynamic Design of Planing Hulls', *Marine Technology, Volume 1, pp. 71-95*, 1964.

Series	L/B	β	C_V
Series 65[7]	3.2-9.26 2.32-9.28	14.8-27.9 16.3-30.4	0 - 3.03 0 - 1.432
Series 62[6]	2.0 -7.0	12.5	0.087-4.116
Metcalf et al.[8]	3.24 – 4.47	16.61, 20	0.28 – 2.634
Fridsma[8,10]	4-6	10-30	0 - 4.0
Zarnick[11]	7,9	10-30	1.57 – 3.15
Southampton (present work)	3.7 – 6.2	22.5	1.75 – 6.77

Table 3: Planing craft systematic series.

Trim [Nm]	Speed [m/s]	C_V	Fr_∇	Fr_L	Re [x10^6]	L_K [m]	L_C [m]	L_M [m]	Z_V [m]	θ_V [°]	R_T [N]	S_V [m^2]
0	4.08±0.1%	2.46±0.2%	2.71±0.1%	1.10±1.3%	5.23±2.6%	1.65±1.5%	1.13±2.2%	1.39±2.5%	-0.03	0.41	18.87±2.3%	0.41±5.2%
0	6.25±0.1%	3.77±0.1%	4.16±0.1%	1.86±1.5%	6.65±3.1%	1.45±1.7%	0.85±2.9%	1.15±3.1%	-0.05	0.72	30.54±1.9%	0.33±6.3%
0	8.13±0.1%	4.91±0.1%	5.41±0.1%	2.58±1.7%	7.61±3.5%	1.35±1.9%	0.68±3.7%	1.01±3.5%	-0.08	0.67	39.87±1.6%	0.29±7.3%
0	10.10±0.1%	6.09±0.2%	6.72±0.1%	3.33±1.9%	8.75±3.8%	1.35±1.9%	0.53±4.8%	0.94±3.8%	-0.09	0.56	51.81±1.4%	0.26±7.9%
0	12.05±0.1%	7.27±0.1%	8.02±0.1%	4.04±2.0%	10.09±3.9%	1.36±1.8%	0.45±5.6%	0.91±3.9%	-0.1	0.56	75.10±1.1%	0.25±8.3%
2.94	4.08±0.2%	2.46±0.2%	2.71±0.2%	1.12±1.3%	5.07±2.7%	1.59±1.6%	1.10±2.3%	1.35±2.6%	-0.01	0.62	17.38±2.5%	0.39±5.3%
2.94	6.25±0.1%	3.77±0.2%	4.16±0.1%	1.94±1.7%	6.14±3.4%	1.35±1.9%	0.78±3.2%	1.06±3.3%	-0.06	0.8	27.68±2.0%	0.30±6.9%
2.94	8.13±0.1%	4.91±0.1%	5.41±0.1%	2.63±1.8%	7.33±3.7%	1.35±1.9%	0.60±4.2%	0.98±3.6%	-0.08	0.72	38.88±1.3%	0.28±7.6%
2.94	10.10±0.1%	6.09±0.1%	6.72±0.1%	3.35±1.9%	8.64±3.9%	1.35±1.9%	0.50±5.0%	0.93±3.8%	-0.09	0.57	55.39±1.0%	0.26±8.1%
2.94	12.05±0.1%	7.27±0.1%	8.02±0.1%	4.11±2.0%	9.75±4.1%	1.35±1.9%	0.40±6.3%	0.88±4.0%	-0.11	0.49	74.65±0.9%	0.24±8.6%
6.87	4.08±0.2%	2.46±0.2%	2.72±0.2%	1.16±1.4%	4.77±2.9%	1.50±1.7%	1.02±2.4%	1.26±2.8%	-0.02	0.57	17.95±2.8%	0.38±5.6%
6.87	6.25±0.1%	3.77±0.1%	4.16±0.1%	1.99±1.8%	5.78±3.6%	1.27±2.0%	0.72±3.4%	1.00±3.5%	-0.08	0.67	26.48±1.9%	0.29±7.3%
6.87	8.13±0.1%	4.91±0.1%	5.41±0.1%	2.70±1.9%	6.96±3.9%	1.27±2.0%	0.57±4.3%	0.92±3.8%	-0.1	0.58	37.57±1.5%	0.26±8.0%
6.87	10.13±0.1%	6.11±0.1%	6.74±0.1%	3.36±1.9%	8.67±3.9%	1.30±1.9%	0.55±4.5%	0.93±3.8%	-0.1	0.44	54.02±1.2%	0.26±8.0%
6.87	12.05±0.1%	7.27±0.1%	8.02±0.1%	4.30±2.2%	8.92±4.5%	1.25±2.0%	0.35±7.1%	0.80±4.4%	-0.11	0.39	70.52±0.9%	0.22±9.5%

Table 4: Model A: calm water data

Trim [Nm]	Speed [m/s]	C_V	Fr_∇	Fr_L	Re [$x10^6$]	L_K [m]	L_C [m]	L_M [m]	Z_V [m]	θ_V [°]	R_T [N]	S_V [m^2]
0	4.08±0.2%	2.27±0.2%	2.54±0.2%	1.13±1.3%	5.00±2.7%	1.55±1.6%	1.10±2.3%	1.33±2.7%	-0	2.06	25.45±2.3%	0.47±5.2%
0	6.25±0.2%	3.47±0.2%	3.90±0.2%	1.95±1.7%	6.07±3.4%	1.33±1.9%	0.78±3.2%	1.05±3.4%	-0.02	4.03	35.22±2.3%	0.36±6.9%
0	8.13±0.1%	4.52±0.1%	5.07±0.1%	2.66±1.9%	7.14±3.8%	1.30±1.9%	0.60±4.2%	0.95±3.7%	-0.02	5.34	49.68±1.7%	0.32±7.7%
0	10.10±0.1%	5.61±0.1%	6.30±0.1%	3.45±2.0%	8.17±4.1%	1.30±1.9%	0.45±5.6%	0.88±4.0%	-0.05	5.22	72.69±1.3%	0.30±8.4%
0	12.05±0.1%	6.70±0.1%	7.52±0.1%	4.24±2.1%	9.20±4.3%	1.30±1.9%	0.35±7.1%	0.82±4.3%	-0.08	0.49	93.56±1.3%	0.28±9.0%
4.74	4.07±0.2%	2.26±0.2%	2.54±0.2%	1.24±1.6%	4.14±3.3%	1.30±1.9%	0.90±2.8%	1.10±3.2%	-0.05	0.76	25.86±4.4%	0.39±6.4%
4.74	6.25±0.1%	3.47±0.2%	3.90±0.1%	2.12±2.0%	5.13±4.0%	1.15±2.2%	0.63±4.0%	0.89±4.0%	-0.08	0.9	36.45±1.8%	0.30±8.2%
4.74	8.15±0.1%	4.53±0.1%	5.09±0.1%	2.82±2.1%	6.41±4.2%	1.20±2.1%	0.50±5.0%	0.85±4.2%	-0.09	0.57	45.69±1.7%	0.29±8.5%
4.74	10.13±0.1%	5.63±0.1%	6.32±0.1%	3.64±2.2%	7.38±4.5%	1.20±2.1%	0.38±6.7%	0.79±4.5%	-0.1	0.54	63.71±1.4%	0.27±9.3%
4.74	12.05±0.3%	6.70±0.3%	7.52±0.3%	4.44±2.4%	8.36±4.8%	1.25±2.0%	0.25±10.0%	0.75±4.7%	-0.09	0.51	89.59±5.7%	0.25±9.9%
9.89	4.08±0.2%	2.27±0.2%	2.55±0.2%	1.16±1.4%	4.75±2.9%	1.49±1.7%	1.02±2.4%	1.26±2.8%	-0.02	0.87	27.49±2.7%	0.45±5.5%
9.89	6.26±0.1%	3.48±0.2%	3.91±0.1%	2.00±1.8%	5.79±3.6%	1.27±2.0%	0.72±3.4%	1.00±3.5%	-0.06	1.22	35.92±2.3%	0.34±7.2%
9.89	8.15±0.1%	4.53±0.1%	5.09±0.1%	2.74±2.0%	6.79±4.0%	1.25±2.0%	0.55±4.5%	0.90±3.9%	-0.08	0.96	49.27±1.8%	0.31±8.1%
9.89	10.13±0.2%	5.63±0.2%	6.32±0.2%	3.48±2.1%	8.08±4.1%	1.27±2.0%	0.45±5.6%	0.86±4.1%	-0.1	0.37	70.24±3.8%	0.29±8.5%
9.89	12.05±0.1%	6.70±0.1%	7.52±0.1%	4.27±2.2%	9.06±4.4%	1.30±1.9%	0.33±7.7%	0.81±4.4%	-0.09	0.96	92.72±1.3%	0.27±9.1%
9.89	10.13±0.1%	5.63±0.1%	6.32±0.1%	3.56±2.1%	7.73±4.3%	1.25±2.0%	0.40±6.3%	0.82±4.3%	-0.08	1.3	67.11±1.5%	0.28±8.9%

Table 5: Model B - calm water data

Trim [Nm]	Speed [m/s]	C_V	Fr_∇	Fr_L	Re [$x10^6$]	L_K [m]	L_C [m]	L_M [m]	Z_V [m]	θ_V [°]	R_T [N]	S_V [m^2]
0	4.05±0.3%	2.07±0.3%	2.39±0.3%	1.16±1.5%	4.64±2.9%	1.45±1.7%	1.02±2.4%	1.24±2.9%	-0.02±7.4%	2.79±0.6%	34.54±3.0%	0.51±5.8%
0	5.09±0.3%	2.60±0.3%	3.01±0.3%	1.58±1.7%	5.00±3.4%	1.30±1.9%	0.82±3.0%	1.06±3.3%	-0.03±3.2%	3.02±0.7%	38.80±3.1%	0.42±6.9%
0	6.23±0.3%	3.19±0.3%	3.68±0.3%	1.98±1.8%	5.79±3.6%	1.28±1.9%	0.72±3.4%	1.00±3.5%	-0.04±3.9%	2.67±0.4%	44.32±2.6%	0.40±7.3%
0	7.11±0.3%	3.63±0.3%	4.20±0.3%	2.31±1.8%	6.37±3.7%	1.27±2.0%	0.66±3.8%	0.97±3.6%	-0.04±3.8%	2.30±0.6%	49.60±2.3%	0.38±7.6%
0	8.13±0.4%	4.16±0.4%	4.81±0.4%	2.67±1.9%	7.10±3.8%	1.30±1.9%	0.59±4.3%	0.94±3.7%	-0.05±1.6%	1.97±1.6%	59.07±1.9%	0.37±7.9%
0	9.21±0.4%	4.71±0.4%	5.44±0.4%	3.12±2.0%	7.56±4.0%	1.30±1.9%	0.47±5.3%	0.89±4.0%	-0.05±2.8%	1.73±1.2%	69.98±2.3%	0.35±8.4%
0	10.10±0.7%	5.16±0.7%	5.97±0.7%	3.47±2.2%	8.06±4.2%	1.30±1.9%	0.42±5.9%	0.86±4.1%	-0.05±5.3%	1.72±1.5%	83.60±1.9%	0.34±8.7%
0	11.13±0.6%	5.69±0.6%	6.58±0.6%	3.80±2.1%	9.01±4.1%	1.35±1.9%	0.40±6.3%	0.88±4.0%	-0.05±1.3%	1.49±2.7%	95.90±2.2%	0.34±8.6%
0	12.05±0.1%	6.16±0.1%	7.12±0.1%	4.17±2.1%	9.48±4.2%	1.35±1.9%	0.35±7.1%	0.85±4.2%	-0.05±1.8%	1.70±2.3%	112.05±1.8%	0.33±8.8%
0	13.09±0.1%	6.69±0.1%	7.73±0.1%	4.57±2.1%	10.14±4.3%	1.35±1.9%	0.33±7.7%	0.84±4.2%	-0.05±2.4%	1.72±2.8%	128.70±3.2%	0.33±9.0%
7.85	4.08±0.3%	2.08±0.3%	2.41±0.3%	1.23±1.6%	4.24±3.2%	1.33±1.9%	0.93±2.7%	1.13±3.1%	-0.02±10.3%	3.04±1.8%	36.70±3.1%	0.47±6.2%
7.85	6.25±0.1%	3.19±0.1%	3.69±0.1%	2.05±1.9%	5.45±3.8%	1.23±2.0%	0.66±3.8%	0.94±3.8%	-0.04±2.9%	2.45±1.4%	44.17±2.6%	0.38±7.7%
7.85	8.13±0.1%	4.16±0.1%	4.81±0.1%	2.74±2.0%	6.77±4.0%	1.25±2.0%	0.55±4.5%	0.90±3.9%	-0.05±1.2%	1.70±2.6%	57.92±2.2%	0.36±8.2%
7.85	10.13±0.1%	5.18±0.1%	5.99±0.1%	3.51±2.1%	7.96±4.2%	1.30±1.9%	0.40±6.3%	0.85±4.2%	-0.05±2.0%	1.33±1.8%	80.73±2.5%	0.33±8.8%
7.85	12.05±0.1%	6.16±0.1%	7.12±0.1%	4.27±2.2%	9.06±4.4%	1.33±1.9%	0.30±8.3%	0.81±4.4%	-0.05±2.2%	1.15±3.0%	108.57±2.1%	0.32±9.2%
14.7	4.08±0.2%	2.08±0.2%	2.41±0.2%	1.19±1.5%	4.52±3.0%	1.40±1.8%	1.00±2.5%	1.20±2.9%	-0.02±3.4%	2.87±0.9%	36.11±2.6%	0.51±5.7%
14.7	6.25±0.1%	3.19±0.1%	3.69±0.1%	1.99±1.8%	5.78±3.6%	1.27±2.0%	0.72±3.4%	1.00±3.5%	-0.04±2.2%	2.55±1.7%	44.90±2.5%	0.40±7.3%
14.7	8.15±0.1%	4.17±0.1%	4.82±0.1%	2.69±1.9%	7.07±3.8%	1.30±1.9%	0.57±4.3%	0.94±3.8%	-0.05±2.5%	1.57±3.6%	59.19±2.3%	0.37±7.9%
14.7	9.87±0.1%	5.04±0.1%	5.83±0.1%	3.35±2.0%	8.08±4.0%	1.31±1.9%	0.46±5.4%	0.89±4.0%	-0.05±3.5%	1.55±1.7%	79.19±2.3%	0.35±8.4%
14.7	12.05±0.1%	6.16±0.2%	7.12±0.1%	4.20±2.1%	9.34±4.3%	1.35±1.9%	0.33±7.7%	0.84±4.2%	-0.05±1.8%	1.38±2.3%	110.79±1.9%	0.33±8.9%

Table 6: Model C - calm water data

Trim [Nm]	Speed [m/s]	Cv	Fr_{∇}	Fr_L	Re [$x10^6$]	L_K [m]	L_C [m]	L_M [m]	Z_V [m]	θ_V [°]	R_T [N]	S_V [m^2]
0	4.07	1.92	2.3	1.19	4.52	1.43±1.8%	0.97±2.6%	1.20±2.9%	-0.01	9.94	51.81±3.0%	0.58±6.0%
0	6.25	2.94	3.52	2	5.75	1.29±1.9%	0.70±3.6%	1.00±3.6%	-0.03	8.09	60.21±2.0%	0.46±7.5%
0	8.13	3.83	4.59	2.7	6.96	1.30±1.9%	0.55±4.5%	0.93±3.8%	-0.03	5.65	76.91±1.9%	0.43±8.1%
0	10.13	4.77	5.71	3.56	7.73	1.35±1.9%	0.30±8.3%	0.83±4.3%	-0.03	4.49	105.18±1.9%	0.38±9.2%
0	12.05	5.67	6.8	4.24	9.2	1.35±1.9%	0.30±8.3%	0.83±4.3%	-0.03	3.87	138.44±2.0%	0.37±9.2%
10.20	4.08	1.92	2.3	1.33	3.63	1.15±2.2%	0.78±3.2%	0.96±3.7%	-0.03	11.53	55.39±3.0%	0.46±7.5%
10.20	6.25	2.94	3.52	2.16	4.94	1.15±2.2%	0.56±4.5%	0.85±4.1%	-0.03	6.11	56.53±3.1%	0.40±8.7%
10.20	8.13	3.83	4.59	2.9	6.02	1.18±2.1%	0.42±5.9%	0.80±4.4%	-0.04	3.47	71.20±2.4%	0.37±9.4%
10.20	10.13	4.77	5.71	3.67	7.26	1.25±2.0%	0.30±8.3%	0.78±4.6%	-0.03	1.99	97.23±2.2%	0.35±9.8%
10.20	12.05	5.67	6.8	4.38	8.58	1.29±1.9%	0.25±10.0%	0.77±4.6%	-0.03	2.77	131.06±1.7%	0.35±9.9%
20.01	4.07	1.92	2.3	1.39	3.29	1.20±2.1%	0.55±4.5%	0.88±4.0%	-0.01	3.02	57.35±2.6%	0.40±8.6%
20.01	6.26	2.95	3.53	2.08	5.36	1.23±2.0%	0.63±4.0%	0.93±3.8%	-0.02	2.48	57.93±3.0%	0.42±8.1%
20.01	8.13	3.83	4.59	2.9	6.02	1.23±2.0%	0.38±6.7%	0.80±4.4%	-0.01	0.4	75.19±2.3%	0.36±9.5%
20.01	10.13	4.77	5.71	3.63	7.43	1.26±2.0%	0.33±7.7%	0.79±4.5%	-0.04	3.48	99.58±2.3%	0.36±9.6%
20.01	12.05	5.67	6.8	4.48	8.22	1.33±1.9%	0.15±16.7%	0.74±4.8%	-0.01	3.59	129.11±1.4%	0.33±10.3%

Table 7: Model D - calm water data

Trim [Nm]	Speed [m/s]	Cv	Fr_∇	Fr_L	Re [$x10^6$]	L_K [m]	L_C [m]	L_M [m]	Z_V [m]	θ_V [°]	R_T [N]	S_V [m^2]
0	4.08±0.3%	2.08±0.3%	2.41±0.3%	1.14±1.4%	4.91±2.8%	1.50±1.7%	1.10±2.3%	1.30±2.7%	-0.02±11.2%	2.34±2.7%	35.60±3.2%	0.56±5.2%
0	6.25±0.3%	3.19±0.3%	3.69±0.3%	1.89±1.6%	6.43±3.2%	1.40±1.8%	0.82±3.0%	1.11±3.2%	-0.04±2.4%	2.60±0.6%	44.36±2.4%	0.44±6.6%
0	8.13±0.3%	4.16±0.3%	4.81±0.3%	2.61±1.8%	7.46±3.6%	1.31±1.9%	0.68±3.7%	0.99±3.6%	-0.05±2.1%	2.22±0.7%	51.25±2.7%	0.39±7.5%
0	10.13±0.5%	5.18±0.5%	5.99±0.5%	3.34±2.0%	8.78±3.8%	1.27±2.0%	0.60±4.2%	0.94±3.8%	-0.05±4.4%	1.93±11.7%	65.97±3.9%	0.37±8.0%
0	12.05±0.8%	6.16±0.8%	7.12±0.8%	4.00±2.1%	10.31±4.0%	1.25±2.0%	0.60±4.2%	0.93±3.8%	-0.06±1.6%	1.72±1.7%	82.31±2.4%	0.36±8.1%

Table 8: Model C1 - calm water data

Trim [Nm]	Speed [m/s]	Cv	Fr_∇	Fr_L	Re [$x10^6$]	L_K [m]	L_C [m]	L_M [m]	Z_V [m]	θ_V [°]	R_T [N]	S_V [m^2]
0	4.05±0.3%	2.07±0.3%	2.40±0.3%	1.14±1.4%	4.81±2.8%	1.49±1.7%	1.08±2.3%	1.28±2.8%	-0.01±10.7%	2.47±3.0%	36.46±2.7%	0.55±5.3%
0	5.10±0.3%	2.61±0.3%	3.01±0.3%	1.51±1.6%	5.46±3.1%	1.38±1.8%	0.94±2.7%	1.16±3.1%	-0.03±7.4%	2.81±1.6%	40.07±3.4%	0.27±10.9%
0	6.25±0.3%	3.19±0.3%	3.69±0.3%	1.93±1.7%	6.17±3.4%	1.31±1.9%	0.82±3.0%	1.07±3.3%	-0.04±2.2%	2.57±0.7%	43.26±3.0%	0.43±6.9%
0	7.11±0.3%	3.63±0.3%	4.20±0.3%	2.26±1.8%	6.66±3.6%	1.27±2.0%	0.75±3.3%	1.01±3.5%	-0.04±2.0%	2.40±1.0%	46.89±2.9%	0.25±11.8%
0	8.13±0.3%	4.16±0.3%	4.81±0.3%	2.62±1.8%	7.39±3.7%	1.29±1.9%	0.68±3.7%	0.98±3.6%	-0.04±2.5%	2.21±1.2%	51.01±2.6%	0.38±7.6%
0	9.18±0.4%	4.69±0.4%	5.43±0.4%	2.99±1.9%	8.18±3.7%	1.27±2.0%	0.65±3.8%	0.96±3.7%	-0.05±2.1%	2.07±2.3%	57.52±3.1%	0.25±11.8%
0	10.13±0.5%	5.18±0.5%	5.99±0.5%	3.34±1.9%	8.78±3.8%	1.27±2.0%	0.60±4.2%	0.94±3.8%	-0.05±1.9%	1.83±1.6%	65.62±2.8%	0.37±8.0%
0	11.13±0.6%	5.69±0.6%	6.58±0.6%	3.77±2.1%	9.14±4.1%	1.27±2.0%	0.50±5.0%	0.89±4.0%	-0.05±2.8%	1.72±2.3%	74.96±2.1%	0.25±11.8%
0	12.05±0.7%	6.16±0.7%	7.12±0.7%	4.03±2.1%	10.17±4.0%	1.27±2.0%	0.55±4.5%	0.91±3.9%	-0.05±1.4%	1.01±2.4%	83.55±2.5%	0.36±8.2%

Table 9: Model C2 - calm water data

Trim [Nm]	Speed [m/s]	Cv	Fr_∇	Fr_L	Re [$x10^6$]	L_K [m]	L_C [m]	L_M [m]	Z_V [m]	θ_V [°]	R_T [N]	S_V [m^2]
0	4.08+0.3%	2.08+0.3%	2.35+0.3%	1.19+1.5%	4.50+3.0%	1.39+1.8%	1.00+2.5%	1.19+3.0%	-0.02+14.9%	3.32+1.5%	42.58+3.1%	0.53+5.6%
0	6.25+0.3%	3.19+0.3%	3.60+0.3%	1.98+1.8%	5.84+3.6%	1.28+1.9%	0.73+3.4%	1.01+3.5%	-0.05+3.0%	2.84+1.5%	49.05+3.7%	0.40+7.2%
0	8.15+0.3%	4.17+0.3%	4.70+0.3%	2.71+1.9%	6.98+3.9%	1.25+2.0%	0.60+4.2%	0.93+3.8%	-0.05+5.8%	*2.61+55.9%*	61.20+2.8%	0.37+7.9%
0	10.13+0.5%	5.18+0.5%	5.84+0.5%	3.43+2.1%	8.32+4.1%	1.30+1.9%	0.47+5.3%	0.89+4.0%	-0.06+2.8%	1.55+1.7%	83.10+3.1%	0.35+8.4%
0	12.05+0.8%	6.16+0.8%	6.95+0.8%	4.19+2.2%	9.39+4.3%	1.33+1.9%	0.36+6.9%	0.84+4.2%	-0.06+1.6%	0.76+103.5%	110.71+3.1%	0.33+8.9%

Table 10: Model C±4 - calm water data

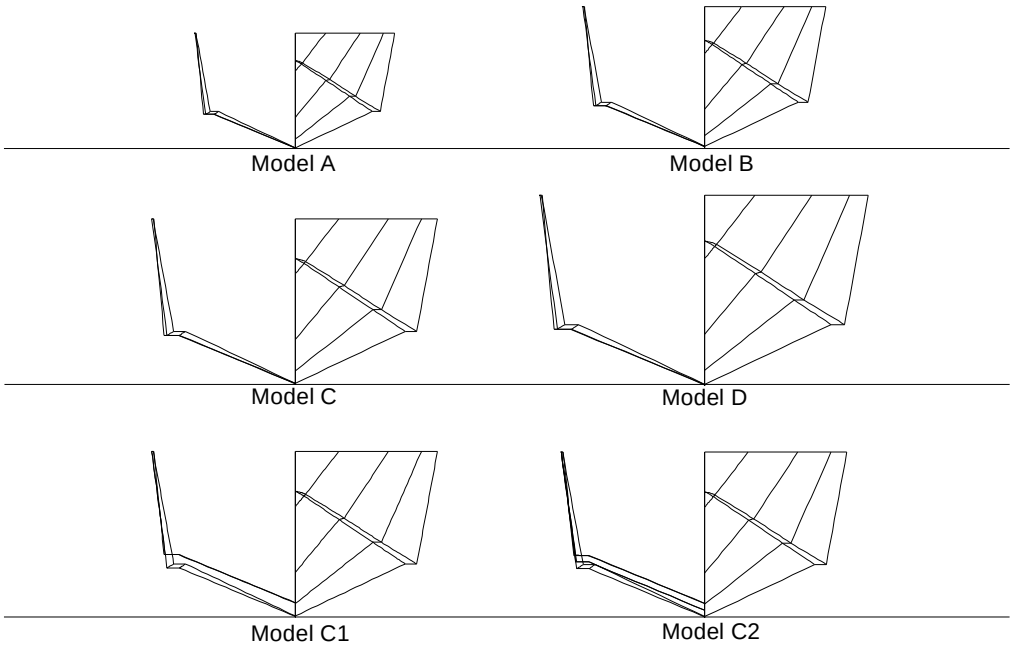

Figure 1: Model body plans.

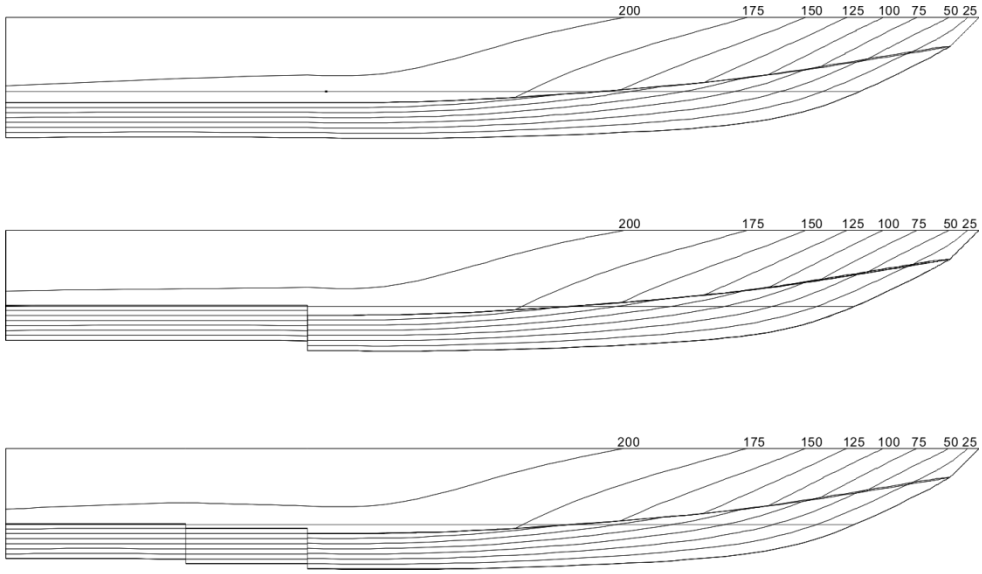

Figure 2: Model profiles (model A-D, model C1, model C2). [Buttock lines in mm]

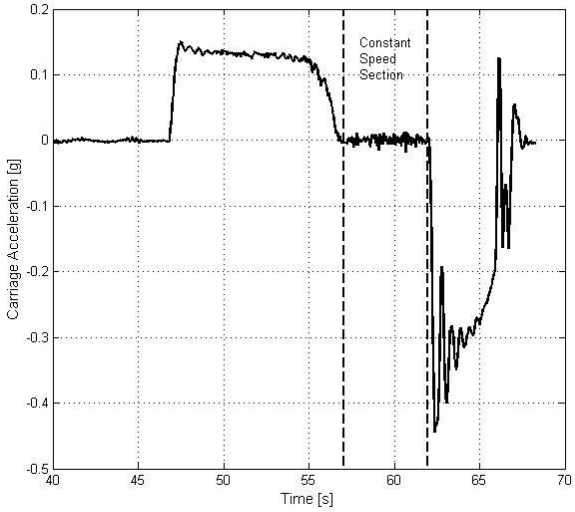

Figure 3: Example carriage acceleration record (for a carriage speed of 12.05 m/s).

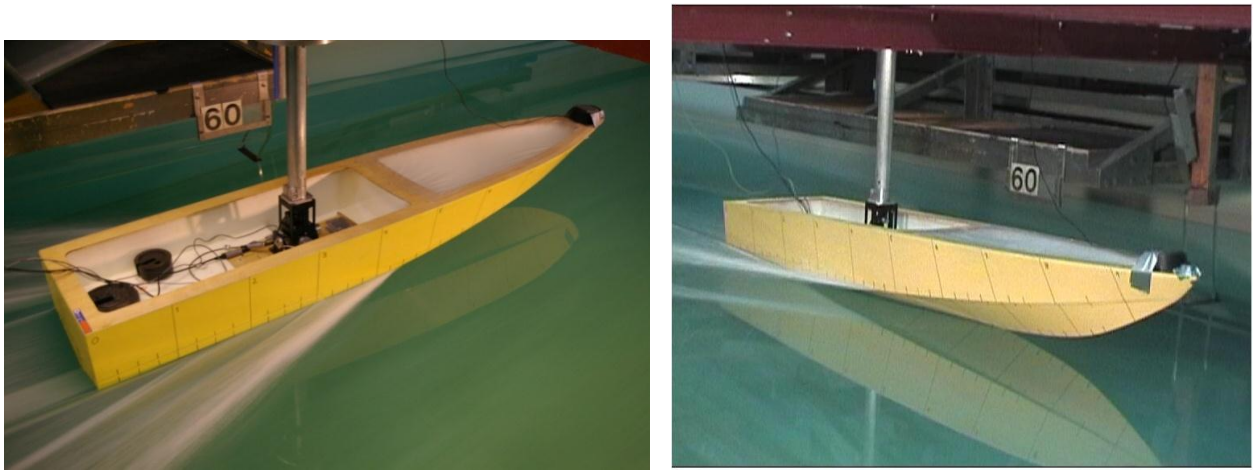

Figure 4: Example of a pair of photographs used to determine the wetted length. The image on the left is used to identify the position where the spray crosses the chine, and the image on the right is used to identify the position where the water contacts the keel. Run shows model C at a speed of 12.05 m/s.

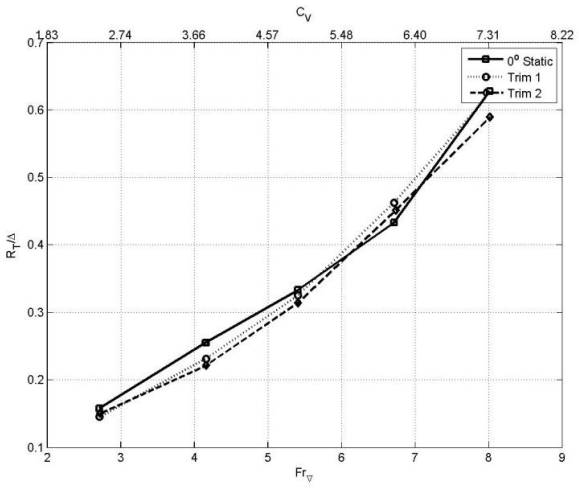

Figure 5: Model A – resistance [trim 1 was produced by a 2.94Nm shift in ballast towards the stern. Trim 2 was produced by a 6.87Nm shift in ballast towards the stern.]

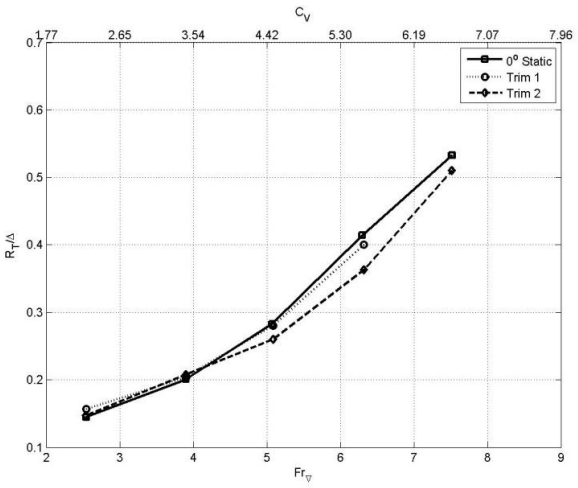

Figure 6: Model B – resistance [trim 1 was produced by a 4.74Nm shift in ballast towards the stern. Trim 2 was produced by a 9.89Nm shift in ballast towards the stern.]

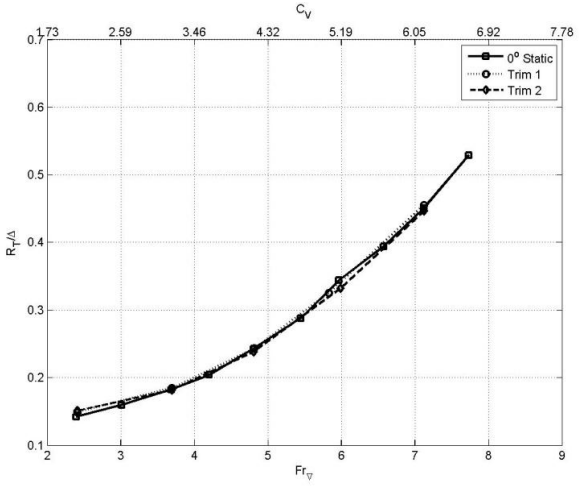

Figure 7: Model C – resistance [trim 1 was produced by a 7.85Nm shift in ballast towards the stern. Trim 2 was produced by a 14.72Nm shift in ballast towards the stern.]

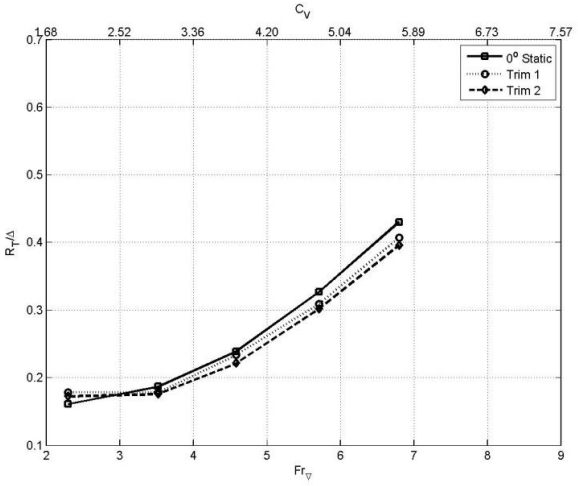

Figure 8: Model D – resistance [trim 1 was produced by a 10.20Nm shift in the ballast towards the stern. Trim 2 was produced by a 20.01Nm shift in the ballast towards the stern.]

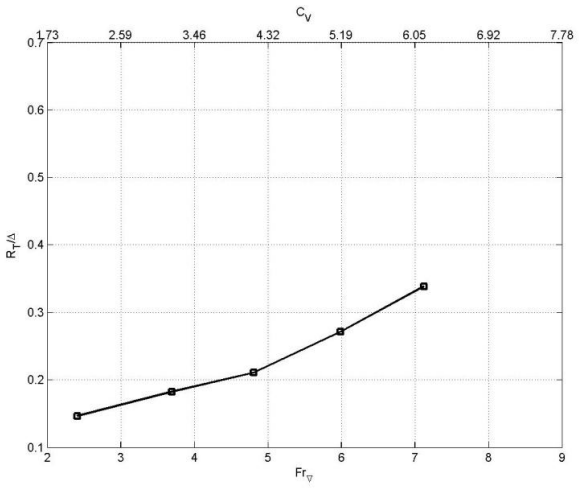

Figure 9: Model C1 - resistance

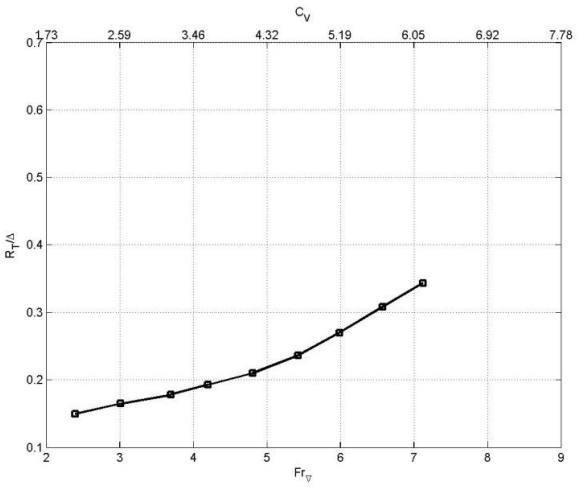

Figure 10: Model C2 - resistance

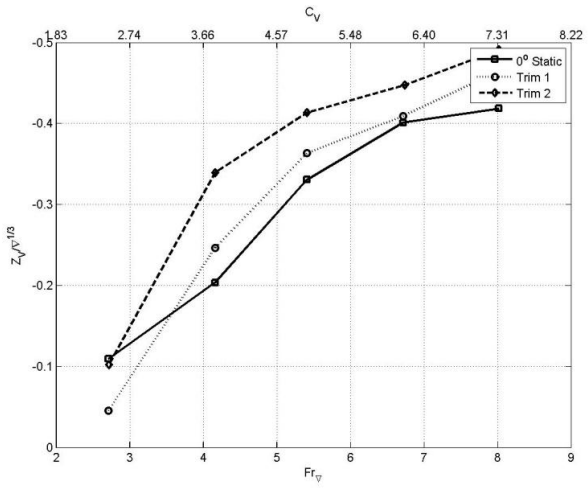

Figure 11: Model A – dynamic sinkage [trim 1 was produced by a 2.94Nm shift in ballast towards the stern. Trim 2 was produced by a 6.87Nm shift in ballast towards the stern.]

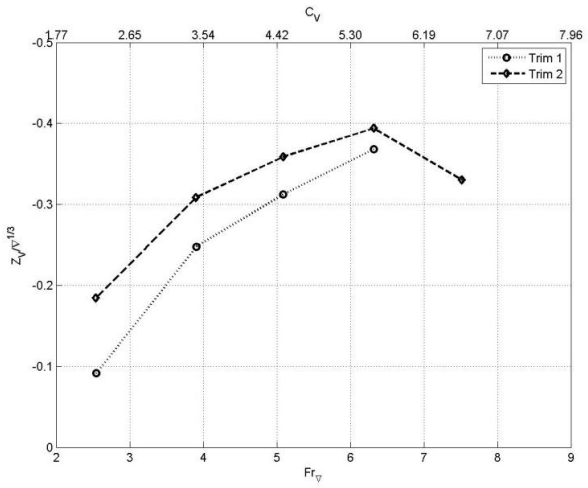

Figure 12: Model B – dynamic sinkage [trim 1 was produced by a 4.74Nm shift in ballast towards the stern. Trim 2 was produced by a 9.89Nm shift in ballast towards the stern.]

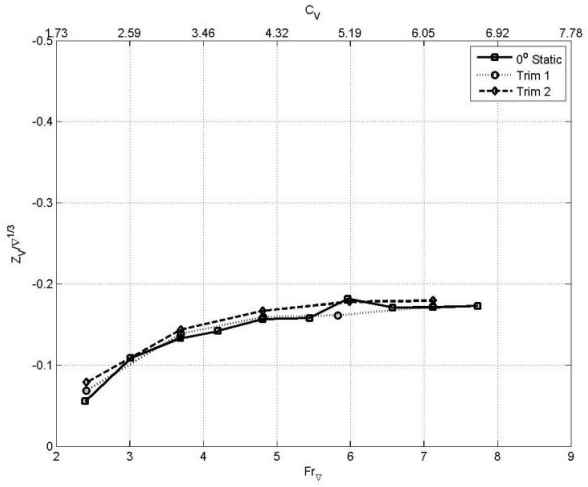

Figure 13: Model C – dynamic sinkage [trim 1 was produced by a 7.85Nm shift in ballast towards the stern. Trim 2 was produced by a 14.72Nm shift in ballast towards the stern.]

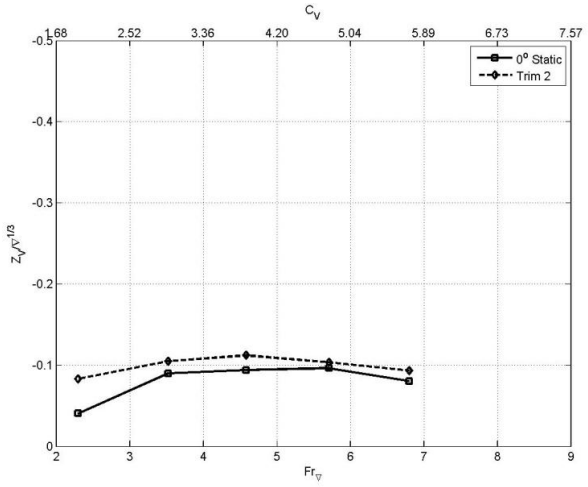

Figure 14: Model D – dynamic sinkage [Trim 2 was produced by a 20.01Nm shift in the ballast towards the stern.]

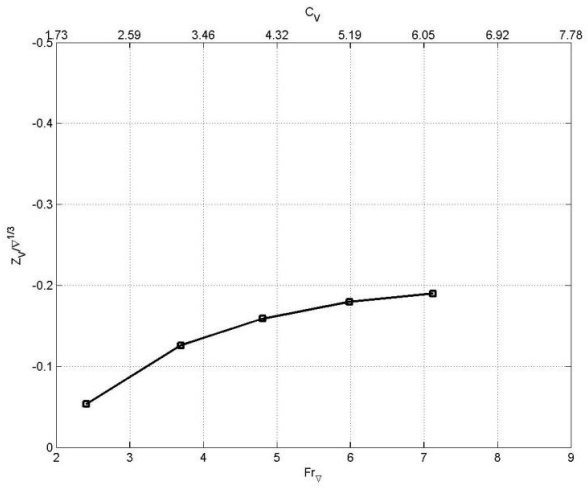

Figure 15: Model C1 – dynamic sinkage

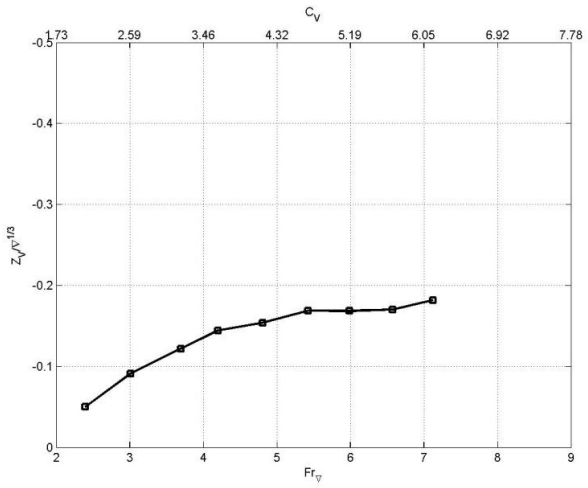

Figure 16: Model C2 – dynamic sinkage

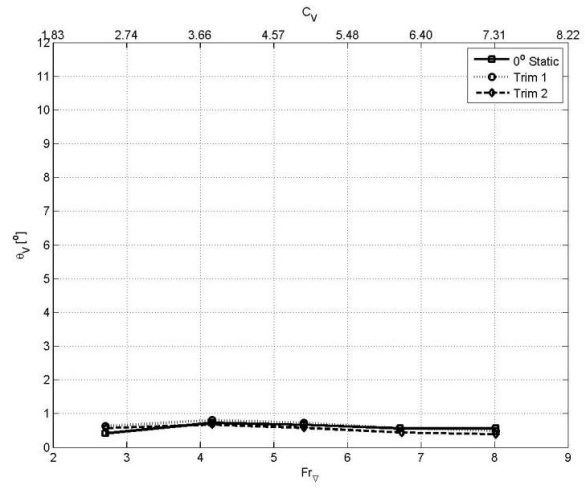

Figure 17: Model A – dynamic trim [trim 1 was produced by a 2.94Nm shift in ballast towards the stern. Trim 2 was produced by a 6.87Nm shift in ballast towards the stern.]

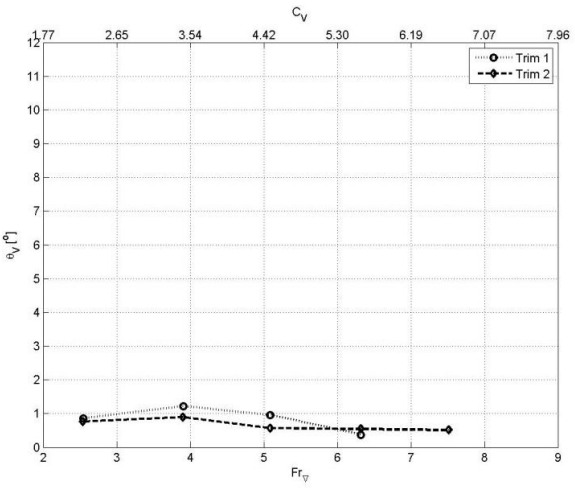

Figure 18: Model B – dynamic trim [trim 1 was produced by a 4.74Nm shift in ballast towards the stern. Trim 2 was produced by a 9.89Nm shift in ballast towards the stern.]

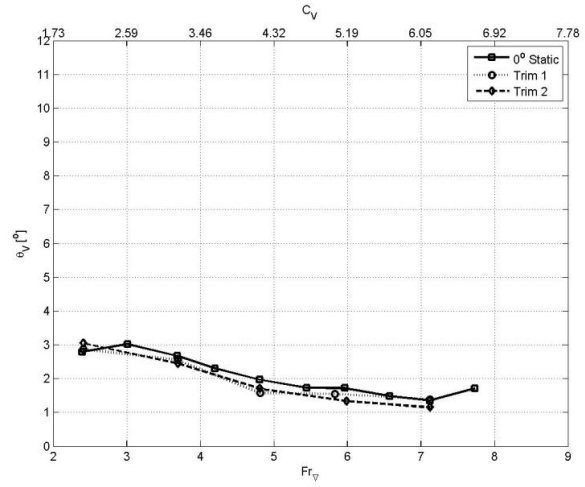

Figure 19: Model C – dynamic trim [trim 1 was produced by a 7.85Nm shift in ballast towards the stern. Trim 2 was produced by a 14.72Nm shift in ballast towards the stern.]

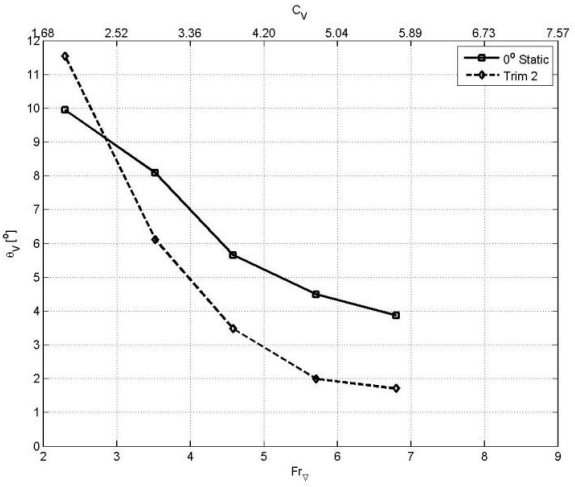

Figure 20: Model D – dynamic trim [Trim 2 was produced by a 20.01Nm shift in the ballast towards the stern.]

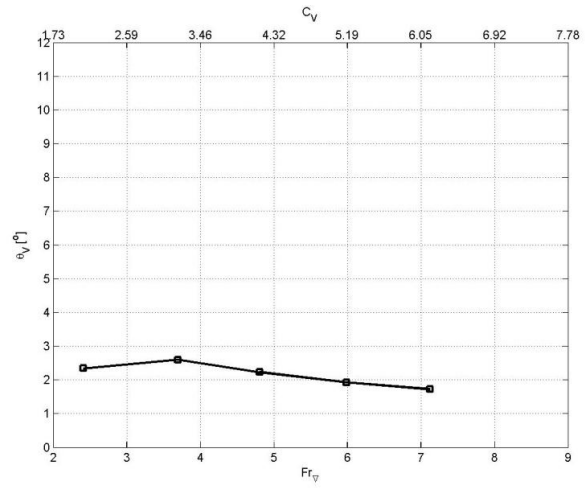

Figure 21: Model C1 – dynamic trim

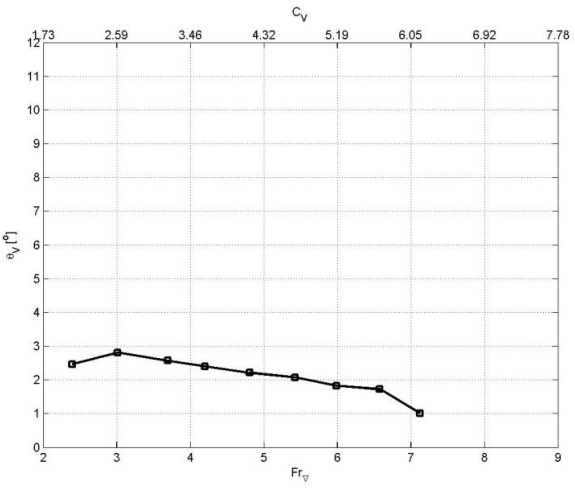

Figure 22: Model C2 – dynamic trim

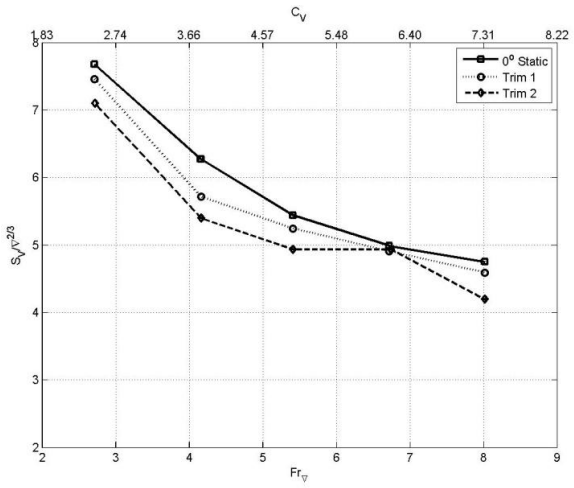

Figure 23: Model A – wetted surface area [trim 1 was produced by a 2.94Nm shift in ballast towards the stern. Trim 2 was produced by a 6.87Nm shift in ballast towards the stern.]

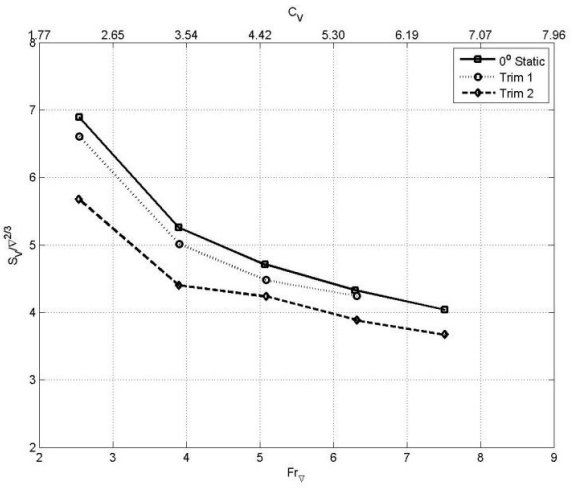

Figure 24: Model B – wetted surface area [trim 1 was produced by a 4.74Nm shift in ballast towards the stern. Trim 2 was produced by a 9.89Nm shift in ballast towards the stern.]

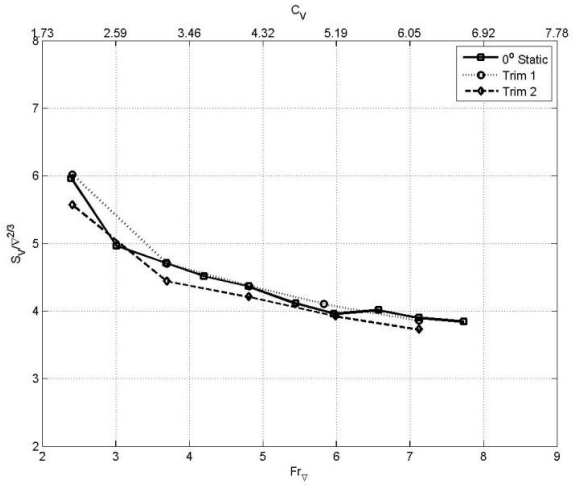

Figure 25: Model C – wetted surface area [trim 1 was produced by a 7.85Nm shift in ballast towards the stern. Trim 2 was produced by a 14.72Nm shift in ballast towards the stern.]

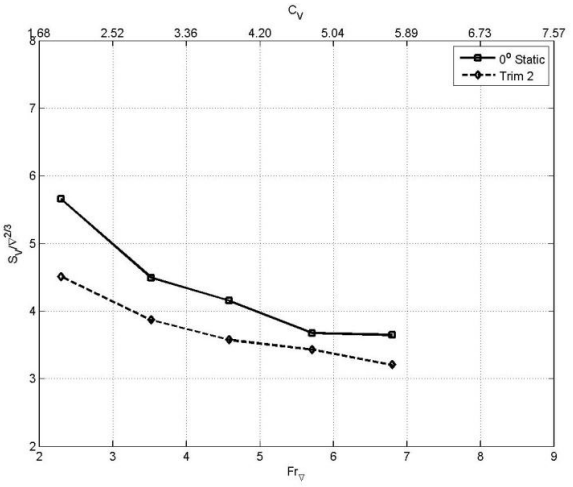

Figure 26: Model D – wetted surface area [Trim 2 was produced by a 20.01Nm shift in the ballast towards the stern.]

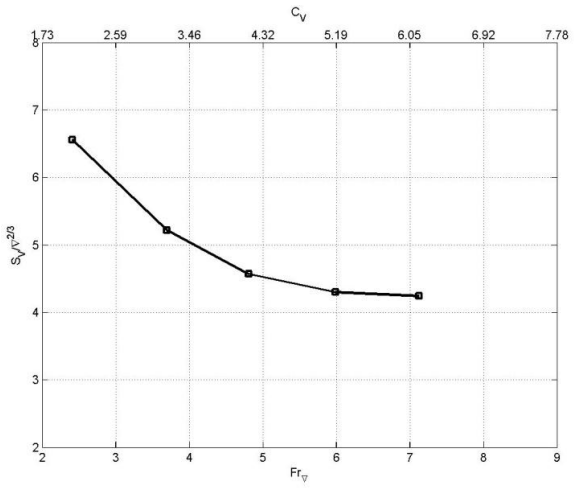

Figure 27: Model C1 – wetted surface area

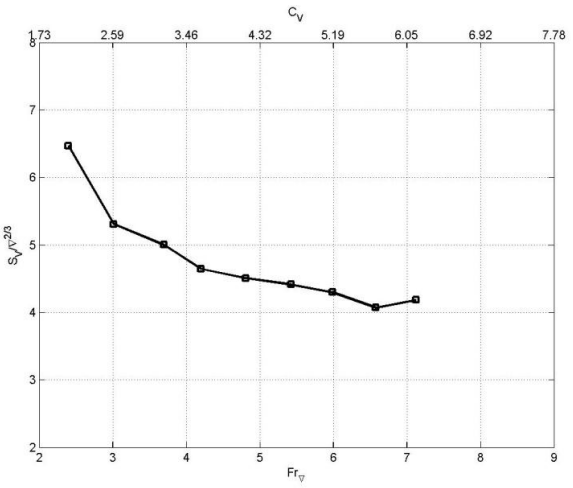

Figure 28: Model C2 – wetted surface area

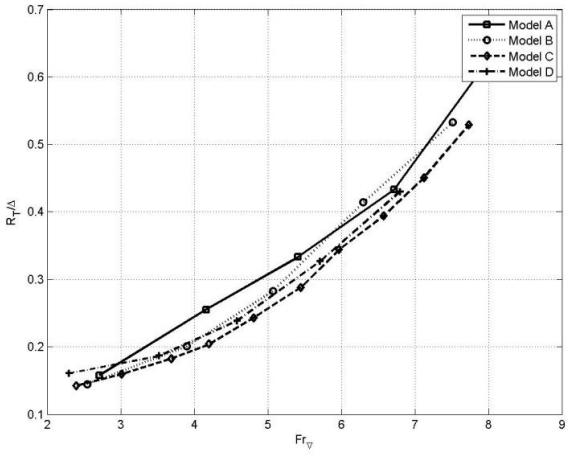

Figure 29: Influence of $L/\nabla^{1/3}$ on resistance

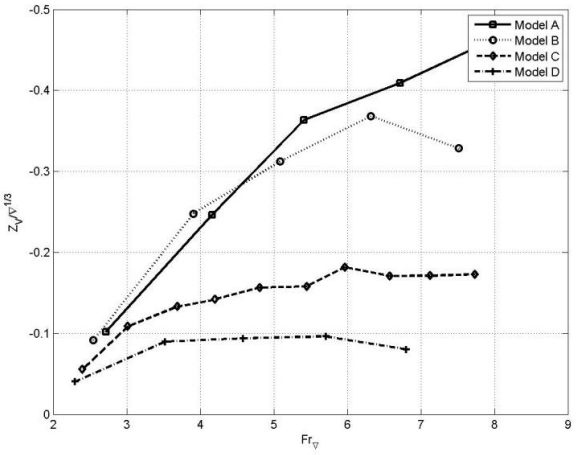

Figure 30: Influence of $L/\nabla^{1/3}$ on dynamic sinkage

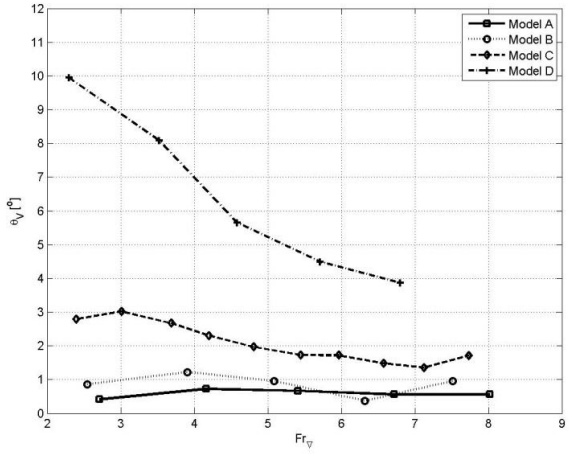

Figure 31: Influence of $L/\nabla^{1/3}$ on dynamic trim [Note: this figure uses the trim condition instead of the static as the results for the static were corrupt].

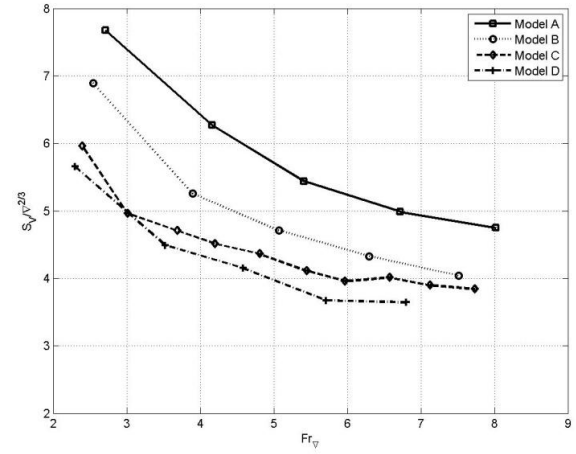

Figure 32: Influence of $L/\nabla^{1/3}$ on wetted surface area

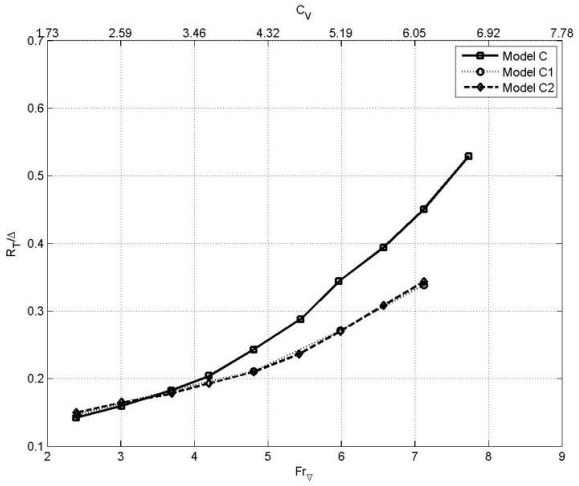

Figure 33: Influence of transverse steps on resistance

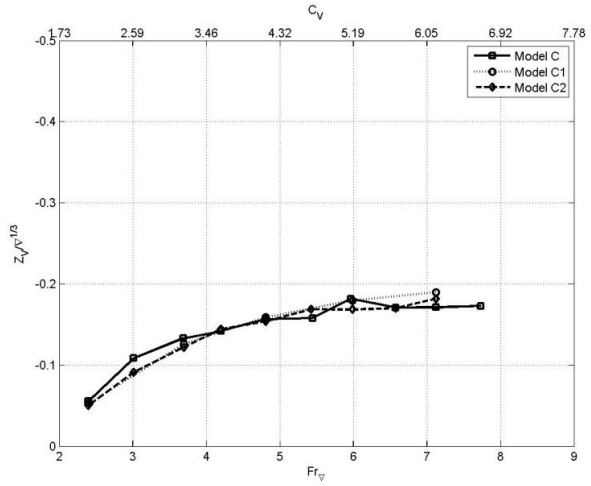

Figure 34: Influence of transverse steps on dynamic sinkage

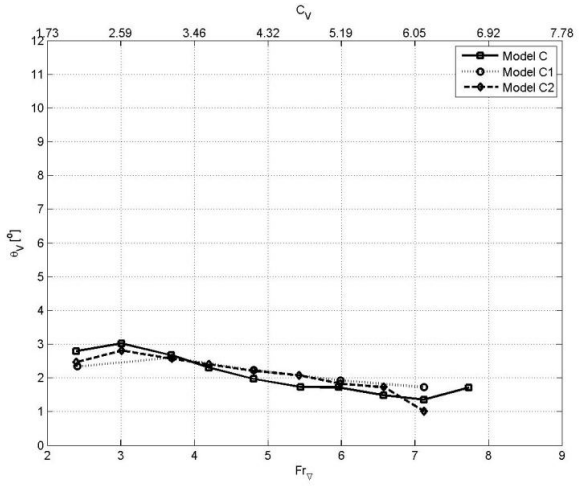

Figure 35: Influence of transverse steps on dynamic trim

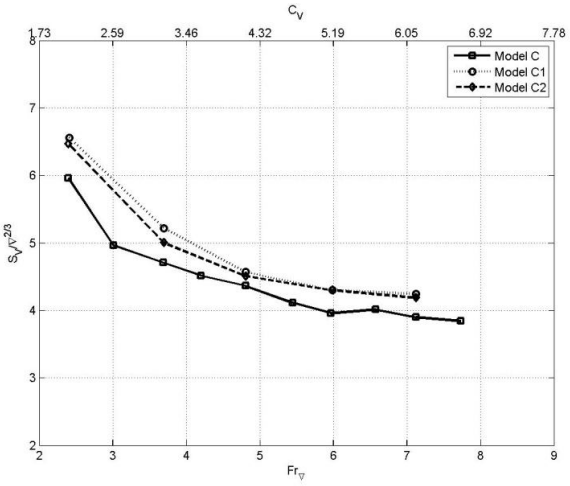

Figure 36: Influence of transverse steps on wetted surface area

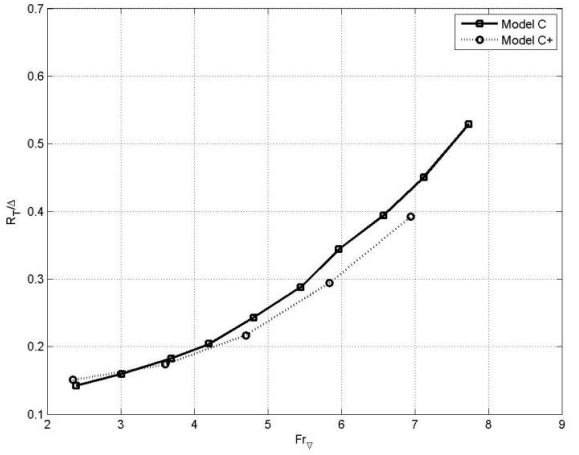

Figure 37: Influence of load coefficient on resistance

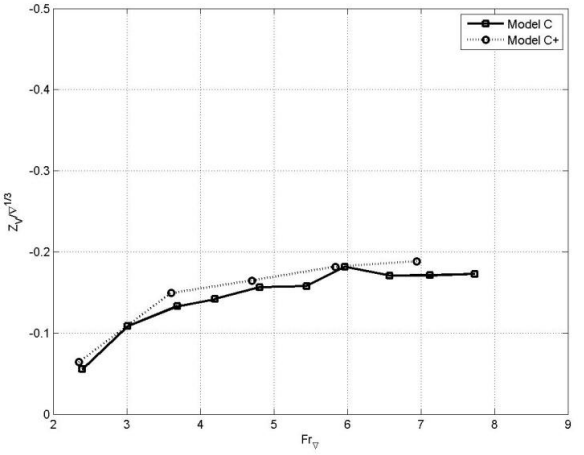

Figure 38: Influence of load coefficient on dynamic sinkage

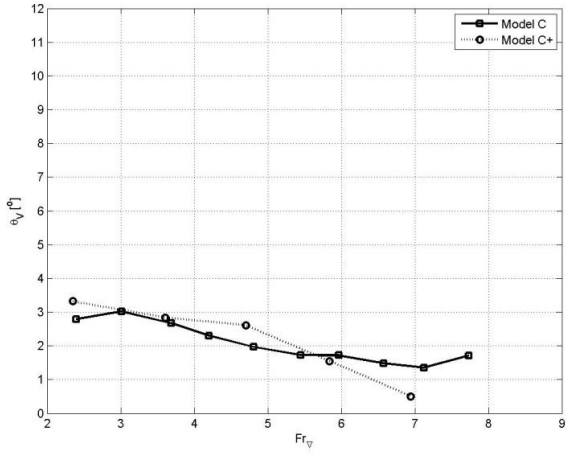

Figure 39: Influence of load coefficient on dynamic trim

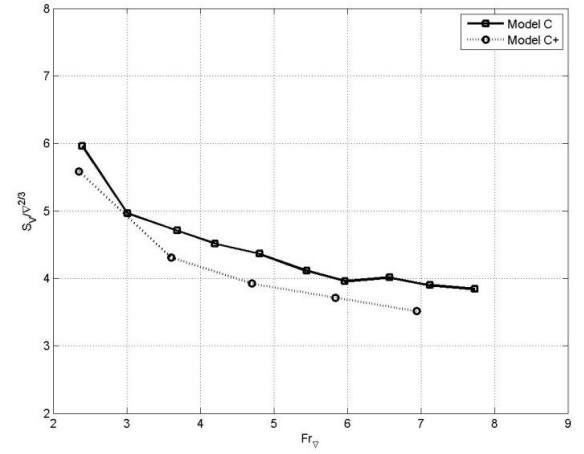

Figure 40: Influence of load coefficient on wetted surface area

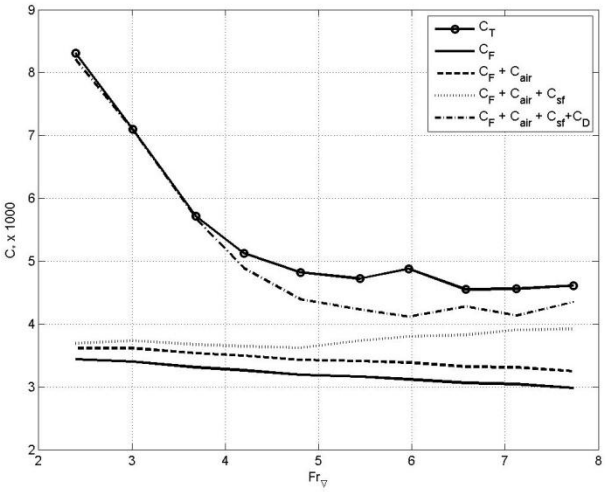

Figure 41: Model C - resistance coefficients